Model Studies on the Mechanism of Deactivation (Exhaustion) of Mixed Oil−Silica Antifoams

Krastanka G. Marinova,[†] Slavka Tcholakova,[†] Nikolai D. Denkov,*[,†] Stoian Roussev,[‡] and Martial Deruelle[§]

Laboratory of Chemical Physics and Engineering, Faculty of Chemistry, Sofia University, 1 James Bourchier Avenue, 1164 Sofia, Bulgaria, Department of Solid State Physics, Faculty of Physics, Sofia University, 5 James Bourchier Avenue, 1164 Sofia, Bulgaria, and Usine Silicones, RHODIA Chimie, CRIT C, 55 Rue des Freres Perret BP 22, 69191 Saint Fons Cedex, France

Received October 27, 2002

1. Introduction

Antifoams are important components of many commercial products, such as detergents, paints, pharmaceuticals, and others.[1] Antifoams are also used in various technologies, such as pulp and paper production, fermentation, and oil processing. It has been shown[2] that mixed liquid−solid antifoams (e.g., those comprising silicone oil and hydrophobic silica) usually have much higher activity than their individual components, if taken separately.

A major problem in the practical application of antifoams is the gradual loss of their activity in the course of foam destruction. This process is termed "antifoam exhaustion" or "deactivation", and several possible explanations have been proposed in the literature.[3−14] Most often, the explanations are as follows: (i) the antifoam globules reduce their size in the course of foam destruction and eventually become too small to rupture efficiently the foam films;[6,8,10] (ii) the antifoam, initially deposited on the surface of the foaming solution, is gradually emulsified and becomes inactive.[7] Other possibilities were discussed in refs 4, 5, and 9 (see also the discussion in ref 12).

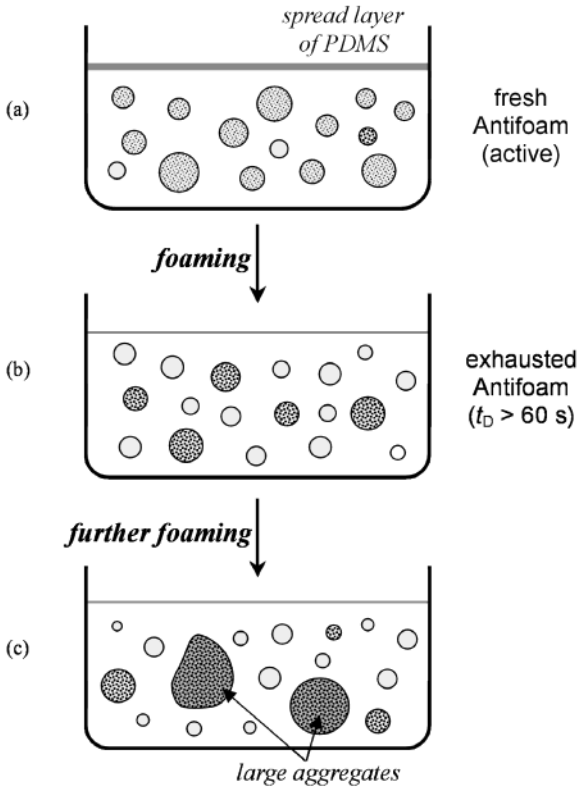

Figure 1. Schematic presentation (adopted from ref 12) of the processes of antifoam exhaustion: (a) An initially active antifoam contains globules of optimal silica/oil ratio; a layer of spread oil is present on the surface of the surfactant solution. (b) The foam destruction by the antifoam globules leads to a gradual segregation of oil and silica into two inactive populations of globules (silica-free and silica-enriched); the spread oil layer disappears from the solution surface, and the antifoam becomes inactive. (c) The process of silica−oil segregation continues on further foaming of the sample, leading to the appearance of larger silica-enriched aggregates.

It was recently shown[12,13] that the exhaustion of mixed poly(dimethylsiloxane) (PDMS)−silica antifoams in surfactant solutions is due to two interrelated processes: (1) segregation of oil and silica into two distinct populations of antifoam globules (silica-free and silica-enriched), both of them being rather inactive; (2) disappearance of the spread oil layer from the solution surface. This mechanism is illustrated in Figure 1: The *oil droplets deprived of silica*, which appear in process 1, are *unable to enter* the surfaces of the foam films and to destroy the foam lamellae, because their entry barrier is too high. Indeed, the existence of a certain critical value of the entry barrier was demonstrated,[14−17] which separates the fast (those that break the foam film) from slow (those unable to enter the foam film surfaces) antifoams. On the other side, the antifoam *globules enriched in silica*, appearing in process 1, are also inactive, because they are *nondeformable* and

* To whom correspondence should be addressed. Phone: (+359) 2-962 5310. Fax: (+359) 2-962 5643. E-mail: ND@LCPE.UNI-SOFIA.BG.

[†] Laboratory of Chemical Physics and Engineering, Sofia University.

[‡] Department of Solid State Physics, Sofia University.

[§] Usine Silicones, RHODIA Chimie.

(1) *Defoaming*: *Theory and Industrial Applications*; Garrett, P. R., Ed.; Marcel Dekker: New York, 1993; Chapters 2−8.

(2) Garrett, P. R. In *Defoaming*: *Theory and Industrial Applications*; Garrett, P. R., Ed.; Marcel Dekker: New York, 1993; Chapter 1.

(3) Exerowa, D.; Kruglyakov, P. M. *Foams and Foam Films*; Elsevier: Amsterdam, 1998; Chapter 9.

(4) Kulkarni, R. D.; Goddard, E. D.; Kanner, B. *Ind. Eng. Chem. Fundam.* **1977**, *16*, 472.

(5) Pouchelon, A.; Araud, A. *J. Dispersion Sci. Technol.* **1993**, *14*, 447.

(6) Koczo, K.; Koczone, J. K.; Wasan, D. T. *J. Colloid Interface Sci.* **1994**, *166*, 225.

(7) Racz, G.; Koczo, K.; Wasan, D. T. *J. Colloid Interface Sci.* **1996**, *181*, 124.

(8) Wasan, D. T.; Christiano, S. P. In *Handbook of Surface and Colloid Chemistry*; Birdi, K. S., Ed.; CRC Press: Boca Raton, FL, 1997; p 179.

(9) Garrett, P. R.; Davis, J.; Rendall, H. M. *Colloids Surf., A* **1994**, *85*, 159.

(10) Bergeron, V.; Cooper, P.; Fischer, C.; Giermanska-Kahn, J.; Langevin, D.; Pouchelon, A. *Colloids Surf., A* **1997**, *122*, 103.

(11) Denkov, N. D.; Cooper, P.; Martin, J.-Y. *Langmuir* **1999**, *15*, 8514.

(12) Denkov, N. D.; Marinova, K. G.; Christova, C.; Hadjiiski, A.; Cooper, P. *Langmuir* **2000**, *16*, 2515.

(13) Marinova, K. G.; Denkov, N. D. *Langmuir* **2001**, *17*, 2426.

(14) Denkov, N. D.; Marinova K. G. *Proceedings of the 3rd Euro-Conference on Foams, Emulsions and Applications*; MIT: Bremen, 2000.

(15) Hadjiiski, A.; Denkov, N. D.; Tcholakova, S.; Ivanov, I. B. In *Adsorption and Aggregation of Surfactants in Solution*; Mittal, K., Shah, D., Eds.; Marcel Dekker: New York, 2002; Chapter 23, pp 465−500.

(16) Basheva, E.; Ganchev, D.; Denkov, N. D.; Kasuga, K.; Satoh, N.; Tsujii, K. *Langmuir* **2000**, *16*, 1000.

(17) Hadjiiski, A.; Tcholakova, S.; Ivanov, I. B.; Gurkov, T. D.; Leonard, E. *Langmuir* **2002**, *18*, 127.

10.1021/la0267589 CCC: $25.00
Published on Web 02/19/2003

the bridging−stretching mechanism[11−13] of foam film rupture cannot be realized. Furthermore, these globules trap some oil which is not readily available for spreading on the solution surface. As a result, the spread layer of silicone oil disappears from the solution surface (process 2) due to oil emulsification in the moment of foam film rupture.

A combination of several experimental methods was applied in ref 12 to prove this mechanism. Dynamic light scattering and optical microscopy were used to show that there was no correlation between the mean size of the antifoam globules and the antifoam activity in the process of exhaustion. The surface tensions of surfactant solutions containing active and completely exhausted antifoams were compared to demonstrate the disappearance of the spread oil layer in the course of exhaustion. On the other side, a quantitative characterization of the main processes, accompanying the exhaustion, was not performed in refs 12 and 13 (except for the globule size measurements), and the respective mechanism was deduced mainly on the basis of qualitative results.

In the present study, we continue with the investigation of the antifoam exhaustion by applying several techniques which give direct quantitative information for the studied processes. Ellipsometry is used to register the changes in the thickness of the layer of spread oil on the surface of the solutions in the course of antifoam exhaustion. In parallel, the film trapping technique (FTT)[15,17] is used to measure the changes in the entry barrier and the deformability of the antifoam globules. The same surfactant (sodium diethylhexyl-sulfosuccinate) and antifoam (mixture of silicone oil and 4.2 wt % hydrophobic silica) are used to complement the previous data[12] and to deepen our understanding of exhaustion. Additionally, we study the properties of a series of antifoam compounds, containing silica of different concentrations, to demonstrate the relation of exhaustion to the segregation of oil from silica.

2. Experimental Details

2.1. Materials. Sodium diethylhexyl-sulfosuccinate, $C_{20}H_{37}O_7SNa$ (AOT, Sigma catalog no. D-0885), is used as a surfactant in the foaming media. Its concentration in the working solutions is 10 mM, which is about 3.5 times the critical micellar concentration (cmc = 2.8 mM). All solutions are prepared with deionized water from a water purification system Milli-Q Organex (Millipore).

As a basic antifoam, we use a mixture (compound) of poly(dimethylsiloxane) oil of dynamic viscosity 1000 mPa s (product of Rhodia Silicones Europe, Saint Fons, France; commercial name 47V1000SH) with 4.2 wt % hydrophobized silica particles R974 of pyrogenic origin (Degussa AG, Germany). The silica particles are produced by flame hydrolysis of silicone tetrachloride.[18] In this process, primary silica spheres with diameter ≈ 12 nm are produced, which partially fuse with one another forming submicrometer-sized, branched aggregates. The mixing of oil and silica is performed under mild stirring at 150 °C for 4 h. The dispersion of silica aggregates in silicone oil leads to formation of larger entities (usually called agglomerates), which have a fractal structure and rather broad size distribution, from 0.1 to 5 μm. Hereafter this dispersion of silica in PDMS is labeled as compound A.

In several sets of experiments, compounds of different silica concentrations (varying from 0.001 to 16 wt %) were studied. First, the most concentrated compound (16 wt %) was prepared by mixing silica R974 and oil 47V1000SH under the conditions specified in the previous paragraph. Afterward, the other compounds were obtained by dilution of the concentrated compound with oil at room temperature.

(18) *Degussa Technical Bulletin Pigments No. 42* (*Synthetic Silicas for Defoamers*), 3rd ed.; Degussa AG: Frankfurt, Germany; 1988.

The antifoam concentration in the foaming solutions was always 0.01 vol %.

2.2. Experimental Methods. 2.2.1. Automated Shake Test (AST). The automated shake tests are performed on a shake-machine Agitest (Bioblock). A 100 mL sample of the foaming solution is placed in a standard 250 mL glass jar, and 10 μL of a compound is introduced into this sample by using a micropipet M800 (Nichiryo Co., Tokyo, Japan), specially designed to supply small volumes of viscous substances. The jar is then mechanically agitated by the Agitest machine, at an amplitude of 2 cm and a frequency of 360 min^{-1}. After each cycle of agitation for 10 s, the solution remains quiescent for another 60 s. During this period, the time required for defoaming of the solution, t_D, is observed; t_D is defined as the time for appearance of a clean water−air interface without bubbles (a shorter defoaming time corresponds to a more active antifoam and vice versa). Afterward, a new shaking cycle is performed and this procedure is repeated until t_D exceeds 60 s in three consecutive cycles, which is considered as the moment of antifoam exhaustion.

2.2.2. Film Trapping Technique. The film trapping technique[15,17,19] is applied to measure the barrier to entry of the antifoam globules. The antifoam globules are captured in an aqueous wetting film on a glass substrate. The drops are observed from below, through the glass substrate, by means of an inverted optical microscope (Jenavert, Carl Zeiss, Germany). When the thickness of the wetting film becomes smaller than the globule diameter, the upper film surface presses the globules against the solid substrate. A meniscus is formed around each globule with a capillary pressure $P_C = (P_A - P_W)$, where P_A is the pressure of the gaseous phase above the film and P_W is the pressure in the aqueous film. P_A is increased by a pressure control system, and the critical capillary pressure, P_C^{CR}, at which the globules enter the air−water interface, is measured (for details see refs 15 and 17). The moment of drop entry, which is accompanied by a significant local change in the meniscus shape, is clearly seen in the microscope. Higher values of P_C^{CR} correspond to more difficult entry and vice versa. For brevity, we term P_C^{CR} as "the entry barrier".

Additionally, this technique allows a microscope examination of the antifoam globules and of the surface of the solutions (e.g., whether a thick layer of oil is spread). The antifoam globules are observed in transmitted light, while the presence of a spread oil layer is detected from the interference pattern appearing in reflected light.

2.2.3. Ellipsometry. The used instrument is a modification[20] of a conventional null type ellipsometer (LEF 3M, Novosibirsk, Russia), which is adapted for kinetic measurements with a time resolution of 1 s. A He−Ne laser (λ = 632.8 nm), equipped with a light polarizer, emits a beam with a certain polarization state. All experiments are performed at an angle of incidence of 50°, which is close to the Brewster angle for water, 53.1°. After reflection from the sample surface, the light changes its polarization and enters the detector (photomultiplier, equipped with a rapidly rotating analyzer). The system is driven by a computer, and the raw data from the detector are instantaneously recomputed to give the two ellipsometric angles Ψ and Δ, as functions of time.[20] From the values of Ψ and Δ, one can calculate the amount of spread oil, Γ (in mg/m^2), and the thickness of the spread layer by using an appropriate optical model. In our calculations, we assumed that the spread oil forms a homogeneous layer of refractive index equal to that of the bulk silicone oil, n_{OIL} = 1.404, sandwiched between air and solution bulk phases with their respective refractive indices. This model gives the thickness of the spread oil layer, d_{EFF}, which is averaged over the observation area, ≈2 mm in diameter, on the solution surface. Numerical simulations showed that the presence of the surfactant adsorption layer slightly affects the calculated value of d_{EFF}, if the assumption is made that the oil spreads without affecting the adsorption layer (according to refs 21 and 22, this assumption is justified for silicone oil spreading on the surface of AOT solutions). Note that the numerical value of d_{EFF} [nm] is

(19) Hadjiiski, A.; Dimova, R.; Denkov, N. D.; Ivanov, I. B.; Borwankar, R. *Langmuir* **1996**, *12*, 6665.
(20) Russev, S. C.; Argirov, T. V. *Rev. Sci. Instrum.* **1999**, *70*, 3077.
(21) Mann, E. K.; Langevin, D. *Langmuir* **1991**, *7*, 1112.
(22) Bergeron, V.; Langevin, D. *Macromolecules* **1996**, *29*, 306.

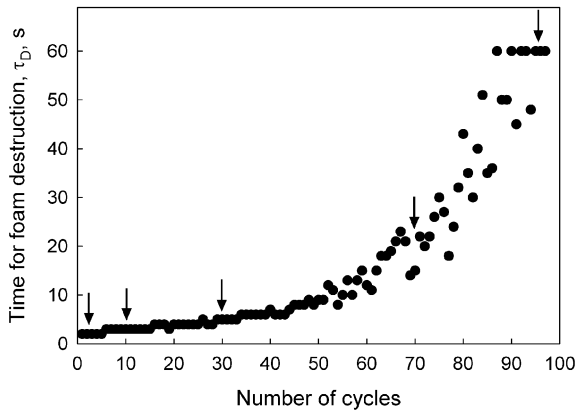

Figure 2. Typical curve of exhaustion of antifoam in aqueous solution of 10 mM AOT. The graph presents the increase of the defoaming time in the presence of 10 μL antifoam compound A with the number of shake cycles.

approximately equal to the value of Γ [mg/m^2], because the mass density of the silicone oil is $\approx 10^3$ kg/m^3.

The experiments were performed as follows: Samples shaken a desired number of cycles in the AST were poured in a Teflon trough (16 × 6 × 1.5 cm). The amount of the oil spread on the solution surface was determined ellipsometrically. Afterward, the oil layer was swept from the surface by a Teflon barrier. The measurement continued another 2 h during which the formation of a new oil layer was detected. The new layer was formed after antifoam globules entered from the bulk onto the surface of the solution. Thus, we were able to determine both the thickness and rate of layer formation on the surface of solutions shaken different numbers of cycles by the AST.

All measurements are performed at room temperature, 20 ± 1 °C.

3. Results and Discussion

3.1. Model Experiments with Compound A. 3.1.1. Exhaustion Profile of the Antifoam Studied by AST. A typical exhaustion curve for compound A in 10 mM AOT solutions is shown in Figure 2. The initial activity (the average defoaming time, t_D, during the first three shaking cycles) is 2 s. The foam destruction remains very fast during the first 50 shaking cycles; t_D is shorter than 10 s. During the next 30 cycles, from the 50th to the 80th cycle, t_D increases from 10 to 30 s. During the last 10 cycles (from the 80th to the 90th), t_D rapidly increases from 30 to more than 60 s, and afterward, the antifoam is considered as exhausted.

It is important to note that a foam destruction for more than 60 s does not mean a complete inhibition of the antifoam activity. The foam formed in the glass jar disappears even after 150 shaking cycles; however, a much longer time is needed for accomplishment of this process. In other words, the accepted criterion for antifoam exhaustion, $t_D = 60$ s, corresponds to a significant reduction but not to a complete suppression of antifoam activity. To mimic a fully exhausted sample, we shook a sample for 300 cycles in the AST; the foam formed in this sample remained stable for more than 10 min after the foaming had been stopped. In sections 3.1.2 and 3.1.3 below, we characterize the changes in the antifoam properties after a certain number of shaking cycles: 3, 10, 30, 70, 95 (see the arrows in Figure 2), and 300 cycles.

It is worthwhile emphasizing that the exhaustion in this system occurs only if there is an actual process of foam destruction. Direct experiments show that the antifoam activity remains practically constant for many hours, if the antifoam is stored dispersed in the foaming solution, without generating foam.

Table 1. Results from the FTT Experiments: Changes in the Properties of the Antifoam Globules in the Course of the Exhaustion Process (cf. Figure 2)

	number of shaking cycles				
	3	30	70	95	300
time for foam destruction, t_D, s	2	4	22	>60	>600
critical pressure to drop entry, P_C^{CR}, Pa	3 ± 2	4 ± 2	9 ± 1	7 ± 2	18 ± 3
fraction of deformable globules, %	100	100	45	26	26
diameter of deformable globules, μm	6−24	7−25	6−25	5−12	3−7
fraction of nondeformable lumps, %	0	0	55	74	74
lump size, μm			6−26	4−50	5−100
thickness of spread oil layer, d_{EFF}, nm (ellipsometry)	250	11	8	2	< 0.5

3.1.2. Critical Pressure for Globule Entry and Deformability of the Antifoam Globules at Different Stages of the Exhaustion Process. The entry barriers of the antifoam globules in the course of antifoam exhaustion were measured by the FTT. In parallel, the fractions of deformable and nondeformable globules in the samples were determined by visual examination in the microscope during the FTT experiments. At least four independent measurements were performed for each system.

The obtained results (see Table 1) show that the number fraction of *deformable globules* significantly decreases in the course of the exhaustion process. The size of these globules remains almost constant, except for the fully exhausted sample, where it is considerably smaller. The critical pressure for entry of these deformable globules increases slowly with the number of the shaking cycle. As demonstrated in section 3.2, this increase of the entry barrier can be explained with the gradual decrease of the concentration of silica particles in the deformable globules.

The remaining objects, observed by the microscope in the shaken samples, are antifoam globules enriched in silica, which behave as *nondeformable lumps* after entrapment in the wetting film; see Figure 3 for an example. The appearance of these lumps corresponds to the onset of the accelerated exhaustion process (60−70th cycle in Figure 2). The microscope observations show that the size of these lumps increases in the course of the exhaustion process. Larger lumps are probably created via flocculation of smaller lumps, during shaking, on the surface of the solution or in the bulk. Apparently, these large aggregates possess high yield stress (due to their high silica content) and do not redisperse upon shaking in the AST. Although these lumps are observed to enter the solution surface at moderate pressures (an entry barrier of 10 Pa is measured for samples shaken 70 and 95 cycles), they cannot rupture the foam films, because the bridging−stretching mechanism requires a significant deformation of the antifoam globules.[11,12]

The above results clearly demonstrate the formation of two types of antifoam globules in the course of the exhaustion process. As shown in section 3.2, compounds containing either silica-deprived or silica-enriched globules have very poor antifoam efficiency.

3.1.3. Change of the Layer of Spread Oil in the Course of Antifoam Exhaustion. The effective thickness of the spread PDMS layer on the surface of AOT solution, containing 0.01 wt % compound A, is shown in Figure 4 as a function of the number of shaking cycles in the AST. Let us note that initially the entire compound (10 μL) is deposited on the surface of the solution, which corresponds to the formation of an initial layer of spread oil with average thickness $d_{EFF} \approx 1$ μm ($\Gamma \approx 10^3$ mg/m^2). However, as seen from Figure 4, a rapid emulsification of

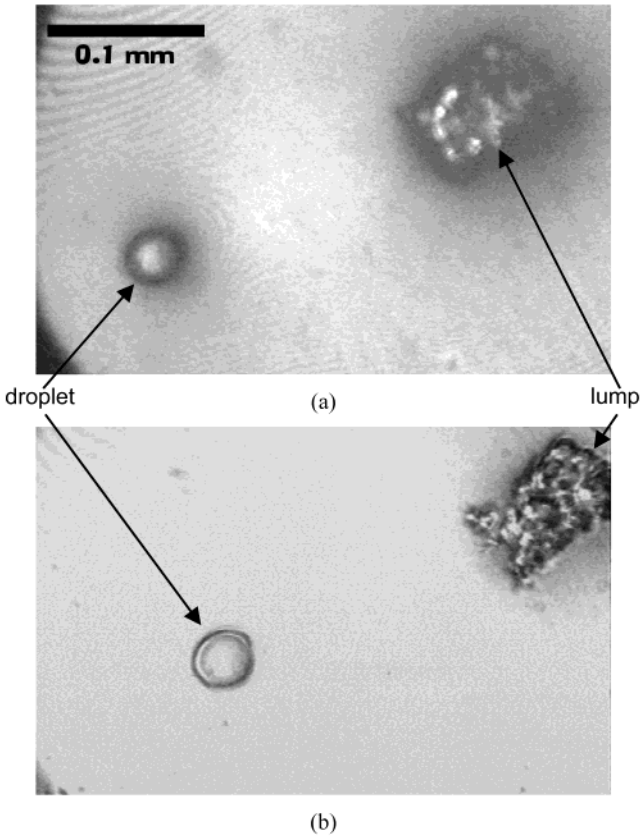

Figure 3. Antifoam globules: deformable droplet and a lump (silica-enriched globule) as seen in reflected (a) and in transmitted (b) light during FTT experiments with samples shaken 95 cycles (0.01% compound A in 10 mM AOT).

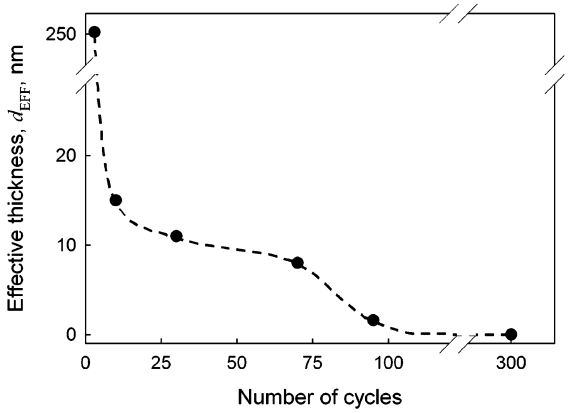

Figure 4. Effective thickness (as determined by ellipsometry) of spread oil on the surface of a 10 mM AOT solution, containing 0.01 wt % of compound A, in the course of antifoam exhaustion in the AST.

this thick spread layer occurs during the first shaking cycles: an oil layer with thickness $d_{EFF} \approx 250$ nm (corresponding to $\Gamma \approx 250$ mg/m^2) remains after 3 shaking cycles, that is, ≈75% of the compound has already been emulsified. Furthermore, the thickness of the spread layer diminishes down to 12 nm after 10 shaking cycles. The latter thickness corresponds to $\Gamma \approx 12$ mg/m^2, which means that only about 1.2% of the total antifoam has remained on the solution surface; that is, almost the entire compound has been emulsified during the first 10 shaking cycles. Nevertheless, the compound is very active at this stage of the exhaustion process.

In the subsequent 50 cycles of shaking, the thickness of the spread layer decreases at a much lower rate (from 12 to 8 nm); see the respective plateau region in Figure 4. During this period, the antifoam is still very active (cf. Figure 2). With the acceleration of the exhaustion process (from the 60th to the 95th cycle, see Figure 2), the thickness of the spread layer decreases rapidly from 8 to 1.5 nm. In the fully exhausted sample, 300 cycles, there is no detectable layer of spread oil on the solution surface.

These results confirm the conclusion drawn in ref 12 that the moments of exhaustion and of disappearance of spread oil from the solution surface are closely related. The role of the spread oil for the process of foam film rupture has been clarified elsewhere: As proven in ref 23 by FTT measurements, the entry barrier of the antifoam globules is significantly lower in the presence of spread oil. Furthermore, as explained in refs 11 and 24, the presence of spread oil facilitates the formation of capillary unstable oil bridges, which rupture the foam films by the bridging−stretching mechanism. In other words, all results obtained with this system (viz., refs 11, 12, 23, and 24 and the present study) indicate that the moment of exhaustion corresponds to the moment of disappearance of the spread oil layer, because the foam film rupture by the antifoam globules is strongly hindered in the absence of spread oil.

The plateau region for the thickness of the spread layer (Figure 4), observed between the 10th and 65th cycles, is explained as a balance of two opposite processes: (1) On one side, the foam film rupture leads to emulsification of some fraction of the oil present on the solution surface. Two possible mechanisms of this emulsification process have been illustrated in Figure 12 of ref 12. (2) On the other side, the active antifoam globules are able to release some spreading oil after entering the solution surface. The shape of the curve in Figure 4 suggests that process 1 (emulsification) prevails during the first cycles (when an excess of antifoam is present on the solution surface) and in the final stage of the exhaustion process (when the oil release from the antifoam globules is hindered for reasons explained below). The plateau region is thus explained as a result of dynamic equilibrium, in which the rates of processes 1 and 2 are almost equal.

To prove our suggestion that some oil reemerges on the solution surface as a result of globule entry, we performed another series of ellipsometric measurements. In these experiments, we studied the kinetics of formation of a new layer of spread oil on a precleaned surface of solutions containing compound A at different levels of exhaustion; see Figure 5. The zero time corresponds to the moment of sweeping the solution surface by the Teflon barrier (section 2.2.3). It is clearly seen that the rate of layer formation, as well the final amount of spread oil, significantly decreases with the advancement of the exhaustion process. A thick oil layer, $d_{EFF} \approx 35$ nm, rapidly forms on the surface of the fresh sample (after 3 cycles), whereas only thin layers, 1 nm or less, slowly form in more exhausted samples (70 or 95 cycles). These results show that the rate of oil appearance on the solution surface, as a result of globule entry (process 2), strongly decreases in the final stage of the exhaustion process. This reduced rate of oil appearance is closely related to the process of silica−oil segregation discussed in the previous subsection: indeed, the silica-deprived globules are unable to supply oil on the solution surface because the entry barrier for them is too high, while the silica-enriched globules are able to release only a very limited amount of oil (and at

(23) Denkov, N. D.; Tcholakova, S.; Marinova, K. G.; Hadjiiski, A. *Langmuir* **2002**, *18*, 5810.
(24) Denkov, N. D. *Langmuir* **1999**, *15*, 8530.

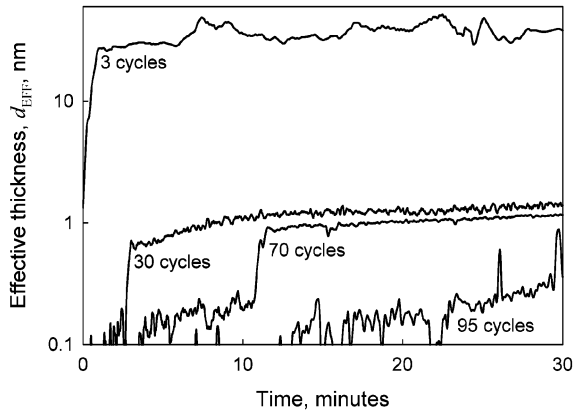

Figure 5. Effective thickness of the spread PDMS layer developing onto the surface of a 10 mM AOT solution as a function of the number of shaking cycles that had been preliminarily applied. Time zero corresponds to the moment of obtaining a clean (from oil) surface after passing the Teflon barrier.

a lower rate); see refs 12 and 26. Note that the nondeformable, silica-enriched globules from the present study resemble in many aspects the gelled compounds which were described in ref 26 (see, e.g., section 3.4 in ref 26 for the process of oil spreading from gelled compounds).

Let us note that the thickness of the layers formed as a result of globule entry during the ellipsometrical experiments, Figure 5, is smaller than the thickness of the layers formed in the shake test, Figure 4. This difference can be explained by taking into account the large dissimilarity between the hydrodynamic conditions (which certainly affect the process of globule entry) in these two types of experiment: the ellipsometrical measurements are performed with a still container, whereas the shake test consists of vigorous agitation of the system. Therefore, one can expect that more antifoam globules are able to enter the solution surface and, respectively, a thicker oil layer is formed in the shake test when other conditions are equivalent.

3.2. Model Experiments with Compounds Containing Various Levels of Silica Particles. In another series of experiments, we studied how the durability (cycles before exhaustion) of PDMS−silica mixtures depends on the silica concentration in the compound. In parallel, we performed FTT experiments with the same compounds to determine the fraction of deformable and nondeformable globules and to measure the barrier to globule entry. The FTT experiments were performed with samples taken after 3 shaking cycles in the AST, to obtain information for globules having the same composition as that of the original (fresh) antifoam compounds.

Figure 6A presents the results for the compound durability (empty circles) as a function of silica concentration. The compounds containing between 1 and 7 wt % of silica had very good durability (>120 cycles). The durability of compounds containing high levels of silica (above 7 wt %) rapidly decreased with silica concentration. The sample containing 0.01 wt % of silica showed poor durability (≈30 cycles), whereas the pure silicone oil without silica and the most diluted compound (0.001 wt % silica) were inactive in the AST.

Figure 6A also presents data for the entry barriers of the compounds (triangles), as measured by the FTT. A

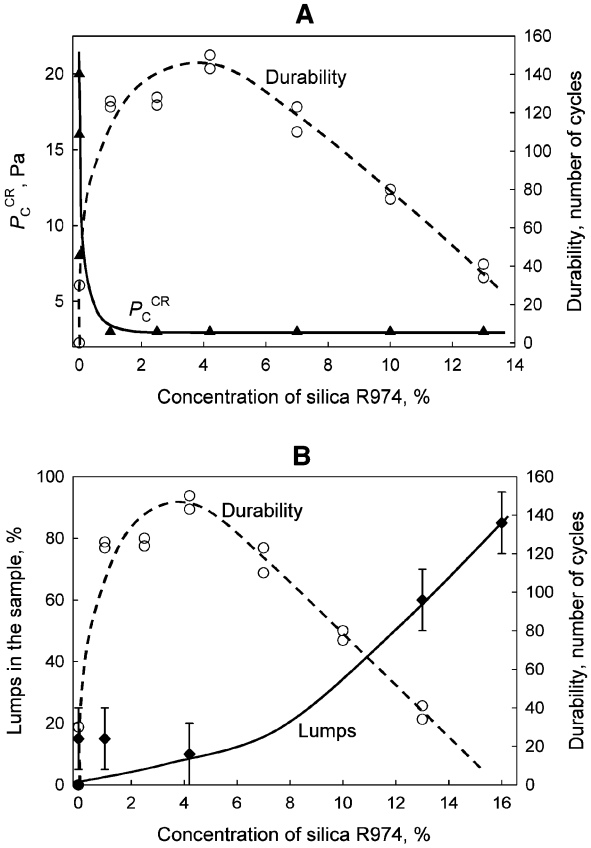

Figure 6. (A) Durability (empty circles connected by dashed curve) and barrier to entry of the deformable droplets (solid triangles connected by solid curve) of compounds containing different concentrations of solid particles. (B) Durability (empty circles connected by dashed curve) and the fraction of nondeformable lumps (diamonds connected by a solid curve) of compounds containing different concentrations of solid particles. The compounds were prepared with silicone oil 47V1000SH and hydrophobic silica R974. The experiments (AST and FTT) were performed with 0.01% compound in 10 mM AOT solution.

clear correlation is seen between the decrease of the entry barrier and the increase of compound durability at low silica concentrations (below 2 wt %). These results confirm once again the important role of the silica particles to reduce the entry barrier[2] and to activate the silicone oil.

On the other side, at higher silica concentrations (>6 wt %), the entry barrier remains low, while a considerable reduction of the antifoam durability is observed (see Figure 6A). As demonstrated in Figure 6B, the durability decrease at high silica content can be easily explained by the significant increase of the fraction of nondeformable lumps in this concentration range. As explained above, these nondeformable lumps are inactive as antifoam entities, because the bridging−stretching mechanism of foam film rupture requires a deformation of the antifoam globules.

The results from this section clearly demonstrated that there is an optimal concentration of silica particles in the compound, which corresponds to maximal durability. Compounds containing silica of too low or too high concentration have poor antifoam efficiency.

4. Conclusions

The process of exhaustion of mixed PDMS−silica antifoams was investigated by several experimental methods, and the main conclusions from the present study are as follows:

The globules in an active fast antifoam are deformable and have a low entry barrier; these are two important

(25) Marinova, K. G.; Denkov, N. D.; Branlard, P.; Giraud, Y.; Deruelle, M. *Langmuir* **2002**, *18*, 3399.
(26) Marinova, K. G.; Denkov, N. D.; Tcholakova, S.; Deruelle, M. *Langmuir* **2002**, *18*, 8761.

requirements for realization of the bridging−stretching mechanism of foam film rupture.[11,24]

The FTT experiments have proven that the process of antifoam exhaustion is related to a gradual segregation of the oil from the silica, which leads to the appearance of two distinct populations of globules: nondeformable (silica-enriched) and deformable (silica-deprived). The deformable globules in the fully exhausted sample (300 cycles) have an entry barrier of 18 ± 3 Pa, which corresponds to a compound containing very low levels of silica (<0.001 wt %). The nondeformable globules present a significant number fraction (≈75%) of all antifoam globules observed in the exhausted samples.

The ellipsometric measurements show that the thickness of the spread oil layer decreases in the course of exhaustion (Figure 4), as a result of oil emulsification in the process of foam destruction. Entering of antifoam globules from the bulk onto the solution surface leads to a partial restoration of the spread layer while the antifoam is still active (see the plateau region in Figure 4). With the advance of the exhaustion process, the oil restoration process is detained and the spread oil disappears due to (1) the increased entry barrier of the deformable globules and (2) the hindered release of oil from the nondeformable globules. The moment of antifoam exhaustion corresponds to a sharp decline in the amount of spread oil on the solution surface.

All these results support and deepen our understanding of the mechanism of antifoam exhaustion, which was proposed in ref 12 (Figure 1).

Acknowledgment. The support of this study and the permission to publish its results by Rhodia Silicones Europe are gratefully acknowledged. The shake tests were performed by Mrs. M. Temelska (Sofia University); her work was very helpful. The interesting and very useful discussions with Dr. Paul Branlard and Dr. Y. Giraud from Rhodia Silicones Europe are also acknowledged.

LA0267589